Journal of Chromatography, 635 (1993) 291-306
Elsevier Science Publishers B.V., Amsterdam

CHROMSYMP. 2655

Capillary electrophoretic chiral separations with cyclodextrin additives

I. Acids: chiral selectivity as a function of pH and the concentration of β-cyclodextrin for fenoprofen and ibuprofen*

Yasir Y. Rawjee, Daniel U. Staerk and Gyula Vigh*

Chemistry Department, Texas A&M University, MS-3255 College Station, TX 77843-3255 (USA)

(First received July 10th, 1992; revised manuscript received November 15th, 1992)

ABSTRACT

An equilibrium model has been developed to describe the pH and cyclodextrin concentration dependence of the electrophoretic mobilities as well as the chiral selectivities observed during the capillary electrophoretic separation of the enantiomers of weak acids. The parameters of the model can be readily derived from three specific sets of capillary electrophoretic experiments cyclodextrin-free background electrolytes of varying pH values are used in the first set of experiments, background electrolytes with the same high pH but varying concentrations of cyclodextrin are used in the second set, and background electrolytes of the same low pH but with varying concentrations of cyclodextrin are used in the third set of experiments. The model has been tested with fenoprofen and ibuprofen as model substances and β-cyclodextrin as resolving agent, and an excellent agreement has been found between the calculated and the measured values. Baseline separations have been achieved for the enantiomers of both fenoprofen and ibuprofen in less than thirty minutes.

INTRODUCTION

Cyclodextrins (CDs) have been used extensively as chiral resolving agents in thin-layer chromatography [1], HPLC [2], GC [3], and recently, in electrophoretic separations [4–22], including micellar electrokinetic chromatography [4–6], isotachophoresis [7–17], free solution capillary electrophoresis (CE) [18–20], and capillary gel electrophoresis [21,22]. Though elegant. chiral CE separations have been achieved with both native α-, β- and γ-cyclodextrins, as well as with peralkylated cyclodextrins, mostly heptakis(2,6-dimethyl-) and heptakis-(2,3,6-trimethyl)-β-cyclodextrins, the operational parameters and background electrolyte compositions which determine the success or failure of a particular separation have not been studied in great detail. Two reports [18,19] indicate that the migration time of a solute increases in a non-linear fashion while peak resolution passes through a maximum as the concentration of the native or derivatized cyclodextrin is increased in the background electrolyte. Another paper [21] used a modified

* Corresponding author.

* Presented at the *16th Znternational Symposium on Column Liquid Chromatography, Baltimore, MD, June 14-19, 1992. The* majority of the papers presented at this symposium were published in *J. Chromutogr.*, Vols. 631 + 632 (1993).

0021-9673/93/$06.00

affinity electrophoresis model to describe chiral selectivity as a function of the cyclodextrin concentration in a capillary gel electrophoretic system that contained β- and y-cyclodextrins incorporated into a polyacrylamide gel matrix. This particular model predicts that the solute migration times increase linearly, while the chiral selectivities increase non-linearly as the cyclodextrin concentration in the gel is increased. However, the effects of other operating parameters, most notably pH, were not studied.

The objective of this series of papers is to examine in detail the effects of the primary CE variables upon the selectivity and the efficiency of chiral CE separations. In this part, the effects of the pH and the concentration of cyclodextrin in the background electrolyte will be studied experimentally using non-steroidal antiinflammatory drugs, ibuprofen and fenoprofen, as model substances. A theoretical model, based on simultaneous multiple equilibria will be presented to account for the observed solute migration times, apparent and true solute mobilities, and chiral selectivities. It will be shown that for the substances studied, the chiral selectivities are at their highest values in low pH background electrolytes (where the acids are hardly dissociated at all), an entirely non-intuitive conclusion considering the coulombic nature of the CE separation process and our knowledge of the chiral separation of profens by HPLC on native β-cyclodextrin silica stationary phases [23].

THEORY

The model

In order to account for the effects of both the pH and the CD concentration of the background electrolyte on the mobility of the individual enantiomers and the resulting chiral separation selectivity, both protonation equilibria and complexation equilibria must be considered simultaneously.

Let us consider a background electrolyte which contains a weak acid, HB, and its conjugate base, B^-, as the buffer components and cyclodextrin, CD, as the chiral resolving agent. The enantiomers of the chiral weak acid analyte to be separated from each other are HR and HS. Let us assume that the analytical concentration of the buffer is much higher than that of either the CD or the enantiomers of the analyte, HR and HS. Cyclodextrin will form complexes with both components of the buffer and the analyte. When the concentration of the buffer is much higher than that of the CD and the concentration of the CD is much higher than that of the analyte, then practically all the CD will be tied up in the CD · buffer complex, unless the complex formation constants are uncharacteristically small. Because the analyte concentration is low with respect to that of the CD, and also, because there is a sufficiently high excess of uncomplexed buffer, the analytical concentration of CD is practically the same as the analytical concentration of the CD · buffer complexes, and remains more or less constant whether the analyte is present or not. Therefore, in a first approximation, the CD-buffer equilibria can be omitted from our considerations. For the sake of simplicity, the terms CD and [CD] will be used *in lieu of* the more proper, but cumbersome terms of CD · buffer complex and its concentration [CD · buffer].

Once in solution, both solute enantiomers, HR and HS, undergo acid dissociation according to eqns. 1 and 2:

$$HR + H_2O \rightleftarrows H_3O^+ + R^- \quad (1)$$

$$HS + H_2O \rightleftarrows H_3O^+ + S^- \quad (2)$$

Cyclodextrin will complex with both the protonated and the deprotonated forms of the analyte enantiomers:

$$HR + CD \rightleftarrows HRCD \quad (3)$$

$$HS + CD \rightleftarrows HSCD \quad (4)$$

$$R^- + CD \rightleftarrows RCD^- \quad (5)$$

$$S^- + CD \rightleftarrows SCD^- \quad (6)$$

The equilibrium expressions which describe these reactions are as follows:

$$K_{HR} = [R^-][H_3O^+]/[HR] \quad (7)$$

$$K_{HS} = [S^-][H_3O^+]/[HS] \quad (8)$$

$$K_{HRCD} = [HRCD]/[HR][CD] \quad (9)$$

$$K_{HSCD} = [HSCD]/[HS][CD] \quad (10)$$

$$K_{RCD^-} = [RCD^-]/[R^-][CD] \quad (11)$$

$$K_{SCD^-} = [SCD^-]/[S^-][CD] \quad (12)$$

The mass balance equations of the HR and the HS related species are, in terms of their analytical concentrations, c_{HR} and c_{HS}:

$$c_{HR} = [HR] + [R^-] + [HRCD] + [RCD^-] \quad (13)$$

$$c_{HS} = [HS] + [S^-] + [HSCD] + [SCD^-] \quad (14)$$

The respective mole fractions of the negatively charged species R^-, RCD^-, S^-, SCD^- are:

$$\alpha_{R^-} = [R^-]/c_{HR} \quad (15)$$

$$\alpha_{S^-} = [S^-]/c_{HS} \quad (16)$$

$$\alpha_{RCD^-} = [RCD^-]/c_{HR} \quad (17)$$

$$\alpha_{SCD^-} = [SCD^-]/c_{HS} \quad (18)$$

An analytical expression can be obtained from eqns. 7-12 for the species concentrations $[R^-]$, $[S^-]$, $[RCD^-]$, and $[SCD^-]$, as well as [HR], [HS], [HRCD], and [HSCD]. Substitution of these expressions into eqns. 13-18 yields:

$$\alpha_{R^-} = \frac{1}{1 + K_{RCD^-}[CD] + \frac{[H_3O^+]}{K_{HR}}(1 + K_{HRCD}[CD])} \quad (19)$$

$$\alpha_{S^-} = \frac{1}{1 + K_{SCD^-}[CD] + \frac{[H_3O^+]}{K_{HS}}(1 + K_{HSCD}[CD])} \quad (20)$$

$$\alpha_{RCD^-} = \frac{K_{RCD^-}[CD]}{1 + K_{RCD^-}[CD] + \frac{[H_3O^+]}{K_{HR}}(1 + K_{HRCD}[CD])} \quad (21)$$

$$\alpha_{SCD^-} = \frac{K_{SCD^-}[CD]}{1 + K_{SCD^-}[CD] + \frac{[H_3O^+]}{K_{HS}}(1 + K_{HSCD}[CD])} \quad (22)$$

The effective mobilities of the two enantiomers can be expressed as the sums of the mole fraction-weighted ionic mobilities of the respective species [24]:

$$\mu_R^{eff} = \mu_{R^-}^0 \alpha_{R^-} + \mu_{RCD^-}^0 \alpha_{RCD^-} \quad (23)$$

$$\mu_S^{eff} = \mu_{S^-}^0 \alpha_{S^-} + \mu_{SCD^-}^0 \alpha_{SCD^-} \quad (24)$$

Combining eqns. 19-22 with eqns. 23-24 we obtain:

$$\mu_R^{eff} = \frac{\mu_{R^-}^0 + \mu_{RCD^-}^0 K_{RCD^-}[CD]}{1 + K_{RCD^-}[CD] + \frac{[H_3O^+]}{K_{HR}}(1 + K_{HRCD}[CD])} \quad (25)$$

$$\mu_S^{eff} = \frac{\mu_{S^-}^0 + \mu_{SCD^-}^0 K_{SCD^-}[CD]}{1 + K_{SCD^-}[CD] + \frac{[H_3O^+]}{K_{HS}}(1 + K_{HSCD}[CD])} \quad (26)$$

or, after factoring out the ionic mobilities of the uncomplexed species, $\mu_{R^-}^0$ and $\mu_{S^-}^0$:

$$\mu_R^{eff} = \frac{1 + \frac{\mu_{RCD^-}^0}{\mu_{R^-}^0} K_{RCD^-}[CD]}{1 + K_{RCD^-}[CD] + \frac{[H_3O^+]}{K_{HR}}(1 + K_{HRCD}[CD])} \quad (27)$$

$$\mu_S^{eff} = \mu_{S^-}^0 \frac{1 + \frac{\mu_{SCD^-}^0}{\mu_{S^-}^0} K_{SCD^-}[CD]}{1 + K_{SCD^-}[CD] + \frac{[H_3O^+]}{K_{HS}}(1 + K_{HSCD}[CD])} \quad (28)$$

It can be seen that the effective solute mobility is a function of the ionic solute mobilities of both the free and the CD complexed species, the acid dissociation constants, the complex formation constants of both the ionic and the non-dissociated forms of the enantiomers, as well as the

pH and the CD concentration of the background electrolyte.

Separation selectivity (chiral selectivity, $A_{R/S}$, in this case) in CE can be expressed as the ratio of the effective mobilities [23]:

$$A_{R/S} = \frac{\mu_R^{eff}}{\mu_S^{eff}} \quad (29)$$

Substitution of eqns. 27-28 into eqn. 29 yields:

$$A_{R/S} = \frac{\mu^0_{R^-}}{\mu^0_{S^-}} \frac{1 + \frac{\mu^0_{RCD^-}}{\mu^0_{R^-}} K_{RCD^-}[CD]}{1 + \frac{\mu^0_{SCD^-}}{\mu^0_{S^-}} K_{SCD^-}[CD]} \frac{1 + K_{SCD^-}[CD] + \frac{[H_3O^+]}{K_{HS}}(1 + K_{HSCD}[CD])}{1 + K_{RCD^-}[CD] + \frac{[H_3O^+]}{K_{HR}}(1 + K_{HRCD}[CD])} \quad (30)$$

As long as the base background electrolyte (*sans* CD) behaves as an isotropic medium, the ionic mobilities of the two enantiomers are identical: $\mu^0_{R^-} = \mu^0_{S^-} = \mu^0_-$. The acid dissociation constants of the two enantiomers are also identical: $K_{HR} = K_{HS} = K_H$. *Thus,* eqn. 30 is simplified to:

$$A_{R/S} = \frac{1 + \frac{\mu^0_{RCD^-}}{\mu^0_-} K_{RCD^-}[CD]}{1 + \frac{\mu^0_{SCD^-}}{\mu^0_-} K_{SCD^-}[CD]} \frac{1 + K_{SCD^-}[CD] + \frac{[H_3O^+]}{K_H}(1 + K_{HSCD}[CD])}{1 + K_{RCD^-}[CD] + \frac{[H_3O^+]}{K_H}(1 + K_{HRCD}[CD])} \quad (31)$$

Eqn. 31 indicates that the chiral selectivity in a CD-based CE system depends on a combination of both thermodynamic parameters (solute specific parameters) and extensive parameters (operator-dependent parameters). The solute specific parameters include the ionic mobilities of the free and the complexed enantiomers (μ^0_-, $\mu^0_{RCD^-}$ and $\mu^0_{SCD^-}$), the acid dissociation constant of the analyte (Ku), the complex formation constants of the ionic enantiomers (K_{RCD^-} and K_{SCD^-}), and the complex formation constants of the protonated enantiomers (K_{HRCD} and K_{HSCD^-}). *The* operator-dependent extensive parameters are the CD concentration and the pH of the background electrolyte.

Discussion of the model

It can be seen from eqn. 31 that in CD-based chiral CE separations chiral selectivity varies according to three fundamentally different situations depending on whether (i) only the non-ionic forms of the two enantiomers, (ii) only the ionic forms of the two enantiomers, or (iii) both forms of the two enantiomers interact differently with CD.

Type Z enantiomers. The separation of Type I enantiomers is the easiest to achieve. Because only the non-ionic forms of the enantiomers interact differently with CD, K_{RCD^-} and K_{SCD^-} are identical. In all probability, $\mu^0_{RCD^-}$ and $\mu^0_{SCD^-}$ are also identical:

$$K_{RCD^-} = K_{SCD^-} = K_{ACD^-} \quad (32)$$

$$\mu^0_{RCD^-} = \mu^0_{SCD^-} = \mu^0_{ACD^-} \quad (33)$$

Thus, the first term of eqn. 31 is reduced to unity, and the $A_{R/S}$ expression is simplified to:

$$A_{R/S} = \frac{1 + K_{ACD^-}[CD] + \frac{[H_3O^+]}{K_H}(1 + K_{HSCD}[CD])}{1 + K_{ACD^-}[CD] + \frac{[H_3O^+]}{K_H}(1 + K_{HRCD}[CD])} \quad (34)$$

It can be seen that the value of the chiral selectivity factor will be different from unity and its magnitude will depend on the values of K_{HRCD}, K_{HSCD}, K_{ACD^-}, K_H, [CD] and pH. If [CD] = 0, $A_{R/S}$ is reduced to unity: there is no chiral separation because the resolving agent, CD, is not present. $A_{R/S}$ changes monotonously as the hydronium ion and the cyclodextrin concentrations are increased. The migration order of the enantiomers cannot be changed by varying either the concentration of CD or the pH. The theoretical chiral selectivity maximum, $A_{R/S} = K_{HSCD}/K_{HRCD}$ can be realized when the "selective complexation" terms (the third term in both

the numerator and the denominator) become much larger than the "parasitic complexation" terms (second term in both the numerator and the denominator) as the concentrations of CD and H_3O^+ are increased ***ad infinitum***. This limiting value can be approximated reasonably closely as soon as

$$\frac{[H_3O^+]}{K_H}(1 + K_{HSCD}[CD]) \geq 100(1 + K_{ACD^-}[CD]) \quad (35)$$

i.e.

$$K_{HSCD} \geq \frac{100K_H - [H_3O^+] + 100K_H}{[H_3O^+][CD] \quad [H_3O^+]} K_{ACD^-} \quad (36)$$

If the hydronium concentration is expressed as a multiple of the acid dissociation constant value,

$$[H_3O^+] = nK_H \quad (37)$$

(***i.e.***, $pH = pK_H -$ log n), then eqn. 36 becomes

$$K_{HSCD} \geq \frac{100 - n}{n[CD]} + \frac{100}{n} K_{ACD^-} \quad (38)$$

By taking [CD] = 15 m*M*, a conservative value that can be safely maintained yet one that is close to the solubility limit of ***β*-CD**, the highest pH values that lead to maximized chiral selectivities at the fastest migration rates can be calculated from eqn. 38. A few representative K_{HSCD}, K_{ACD^-} and pH combinations are listed in Table I. The minimum K_{HSCD} requirement outlined in rows 1 and 2 of Table I is often fulfilled for Type I chiral acids ***(vide infra)*** resulting in a simple expression for chiral selectivity:

$$A_{R/S} = \frac{1 + K_{HSCD}[CD]}{1 + K_{HRCD}[CD]} \quad (39)$$

These considerations explain the surprising, non-intuitive, but valid observation that in certain CE separations of chiral weak acids, chiral selectivity increases with decreasing pH, because the parasitic non-selective complexation of the ionic enantiomers is reduced as the ionic species is gradually turned into the selectively complexing nonionic species. In the case of Type I enantiomers there is no reversal in the migration order, ***i.e.*** A_{RIS} ***only*** varies between unity and its maximum value. This makes optimization of the separation simple: the pH of the background electrolyte must be decreased until the selectivity becomes sufficiently high so that the desired peak resolution is realized with the available separation efficiency resulting, automatically, in the shortest possible separation time. Any pH lower than that will result in very rapidly increasing separation time.

TABLE I

REPRESENTATIVE COMPLEXATION CONSTANT AND MAXIMUM pH VALUE PAIRS LEADING TO MAXIMUM CHIRAL SELECTIVITY FOR TYPE I AND TYPE II WEAK ACIDS

n	pH	Type I acid, minimum K_{HSCD} at [CD] = 15 m*M*	Type II acid, minimum K_{HACD} at [CD] = 15 m*M*
1000	$pK_H - 3$	$0.1K_{ACD^-} - 60$	$0.1K_{SCD^-} - 60$
100	$pK_H - 2$	K_{ACD^-}	K_{SCD^-}
10	$pK_H - 1$	$600 + 10K_{ACD^-}$	$600 + 10K_{SCD^-}$
1	pK_H	$6600 + 100K_{ACD^-}$	$6600 + 100K_{SCD^-}$

Type ZZ enantiomers. The separation of Type II enantiomers is more difficult to achieve. Because only the dissociated forms of the enantiomers interact differently with CD, K_{HRCD} and K_{HSCD} are identical:

$$K_{HRCD} = K_{HSCD} = K_{HACD} \quad (40)$$

$\mu^0_{RCD^-}$ and $\mu^0_{SCD^-}$ may be equal or different, depending on the volume of the respective ionic enantiomer · CD complex. Thus, eqn. 35 is simplified only slightly:

$$A_{RIS} = \frac{1 + \frac{\mu^0_{RCD^-}}{\mu^0_-} K_{RCD^-}[CD]}{1 + \frac{\mu^0_{SCD^-}}{\mu^0_-} K_{SCD^-}[CD]} \cdot \frac{1 + K_{SCD^-}[CD] + \frac{[H_3O^+]}{K_H}(1 + K_{HACD}[CD])}{1 + K_{RCD^-}[CD] + \frac{[H_3O^+]}{K_H}(1 + K_{HACD}[CD])} \quad (41)$$

Note that the ***R*** enantiomer related values are in the numerator in the first term and in the denominator in the second term of eqn. 41. Therefore, $A_{\prime\prime\prime} < 1$, $A_{R/S} = 1$, and $A_{\prime\prime\prime} > 1$ are possible depending on the relative values of the equilibrium constants and the ionic mobilities, as well as the hydronium and the cyclodextrin concentrations. This also means that the migration order of the enantiomers can be reversed by varying the concentrations of the CD and the hydronium ion.

For Type II enantiomers chiral selectivity can be maximized by forcing the entire second term in eqn. 41 to assume a value of unity. This can be achieved by increasing the value of the non-selective complexation term relative to the selective complexation term by increasing the concentration of the hydronium ion, ***i.e.:***

$$\frac{[H_3O^+]}{K_H}(1 + K_{HACD}[CD]) \geq 100(1 + K_{SCD^-}[CD]) \quad (42)$$

or

$$K_{HACD} \geq \frac{100K_H - [H_3O^+] + 100K_H}{[H_3O^+][CD] \quad [H_3O^+]} K_{SCD^-} \quad (43)$$

If the hydronium concentration is once again expressed as a multiple of the acid dissociation constant value as in eqn. 37 ***(i.e.*** $pH = pK_H - \log n$), eqn. 43 becomes:

$$K_{HACD} \geq \frac{100 - n}{n[CD]} + \frac{100}{n} K_{SCD^-} \quad (44)$$

Except for the different subscripts, this relation is formally analogous to the one in eqn. 38. By taking once again [CD] = 15 m***M***, the highest **pH** values that lead to maximized chiral selectivities for Type II acids can be calculated from eqn. 44. A few representative K_{HACD}, K_{SCD^-} and **pH** combinations are listed in Table I. Once again, the minimum K_{HACD} requirement shown in rows 1 and 2 of the last column of Table I is easily **fulfilled** for Type II chiral acids (see below) resulting in a reasonably simple expression for chiral selectivity:

$$A_{R/S} = \frac{1 + \frac{\mu^0_{RCD^-}}{\mu^0_-} K_{RCD^-}[CD]}{1 + \frac{\mu^0_{SCD^-}}{\mu^0_-} K_{SCD^-}[CD]} \quad (45)$$

Again, these considerations explain the surprising, non-intuitive, but valid observation that in certain CE separations of chiral weak acids, chiral selectivity increases with decreasing **pH.** However, chiral selectivities are generally lower than those seen for Type I acids, because unlike in eqn. 39, the selective complexation terms (K_{RCD^-}[CD] and K_{SCD^-}[CD]) are now multiplied by the mobility ratios ($\mu^0_{RCD^-}/\mu^0_-$ and $\mu^0_{SCD^-}/\mu^0_-$), which are generally around 0.1 or lower due to the larger size of the cyclodextrin-complexed enantiomer. This decreases the effect of the selective complexation terms with respect to 1 both in the numerator and the denominator. Optimization of the separation is still simple: the **pH** of the background electrolyte must be decreased until the selectivity becomes sufficiently high so that the desired peak resolution is realized with the available separation efficiency.

However, in the case of Type II acids, there is another alternative that could lead to chiral resolution, namely one could suppress the **pH** dependent part of second term in eqn. 41. This would occur when

$$1 + K_{SCD^-}[CD] \geq 100 \frac{[H_3O^+]}{K_H}(1 + K_{HACD}[CD]) \quad (46)$$

that is, when

$$K_{SCD^-} \geq \frac{100[H_3O^+] - K_H + 100[H_3O^+]}{K_H[CD] \quad K_H} K_{HACD} \quad (47)$$

Using the same $[H_3O^+] = nK_H$ approach as before, eqn. 47 becomes:

$$K_{SCD^-} \geq \frac{100n - 1}{[CD]} + 100nK_{HACD} \quad (48)$$

By taking [CD] = 15 m***M,*** the lowest **pH** values that also lead to alternative maximized chiral selectivities, albeit possibly at altered migration orders, can be calculated from eqn. **48.** A few

TABLE II

REPRESENTATIVE COMPLEXATION CONSTANT AND MINIMUM pH VALUE PAIRS LEADING TO ALTERNATIVE MAXIMUM CHIRAL SELECTIVITIES FOR TYPE II WEAK ACIDS

n	pH	Minimum K_{SCD^-} at [CD] = 15 m*M*
1	pK_H	$6600 + 100K_{HACD}$
0.1	$pK_H + 1$	$600 + 10K_{HACD}$
0.01	$pK_H + 2$	K_{HACD}
0.001	$pK_H + 3$	$0.1K_{HACD} - 60$

representative K_{HACD}, K_{SCD^-} and pH combinations are listed in Table II. Only the minimum K_{SCD^-} requirement shown in the last row of Table II is likely to occur in practice. In this case the expression for chiral selectivity becomes:

$$A_{RIS} = \frac{1 + \frac{\mu^0_{RCD^-}}{\mu^0_-} K_{RCD^-}[CD]}{1 + \frac{\mu^0_{SCD^-}}{\mu^0_-} K_{SCD^-}[CD]} \cdot \frac{1 + K_{SCD^-}[CD]}{1 + K_{RCD^-}[CD]} \quad (49)$$

Because the less-than-unity mobility ratio multipliers ($\mu^0_{RCD^-}/\mu^0_-$ and $\mu^0_{SCD^-}/\mu^0_-$) are absent in the second term of eqn. 49, chances are that the A_{RIS} value will be dominated by the second term meaning that in the high pH background electrolyte the migration order of the enantiomers will be reversed with respect to the one observed at low pH. However, unless this reversal is very important for a particular analysis, the use of the high pH background electrolyte is disadvantageous, because the two terms in eqn. 49 counteract each other resulting in a chiral selectivity that is lower than what could have been achieved in the low pH electrolyte (eqn. 45).

Type ZZZ *enantiomers*. The separation of Type III enantiomers is the most difficult of all to predict. Because both the dissociated 'and non-dissociated forms of the enantiomers interact differently with CD, eqn. 31 cannot be simplified and an a *priori* selection of the "best" background electrolyte pH is not possible. The migration order may change as either the pH or the CD concentration is varied. These reversals, as well as the actual selectivities, depend on the particular set of complex formation constants and ionic mobilities. A detailed study of the pH is essential if the optimum separation conditions are to be determined. However, from a practical point of view, the use of a low-pH electrolyte seems the most promising approach, because this would maximize the value of the second term in eqn. 31.

Determination of the model parameters

Generally, only μ^0_- and K_H *are* available of the model parameters, if at all. However, reasonable parameter estimates can be obtained from specifically designed sets of experiments and a few simple assumptions, as follows.

If there is no cyclodextrin in the background electrolyte, then the effective ionic mobilities and the acid dissociation constants of the two enantiomers are identical and both can be determined from electropherograms taken at different pH values. Specifically, when [CD] = 0, eqns. 27 and 28 are simplified to eqn. 50:

$$\frac{\mu^{eff}_-}{\mu^0_-} = \frac{\mu^{eff}_R}{\mu^0_{R^-}} = \frac{\mu^{eff}_S}{\mu^0_{S^-}} = \frac{1}{1 + \frac{[H_3O^+]}{K_{HR}}} = \frac{1}{1 + \frac{[H_3O^+]}{K_{HS}}} = \frac{K_H}{K_H + [H_3O^+]} \quad (50)$$

or:

$$\frac{1}{\mu^{eff}_-} = \frac{1}{\mu^0_-} + \frac{[H_3O^+]}{\mu^0_- K_H} \quad (51)$$

from which the μ^0_- and the K_H values can be determined by plotting $1/\mu^{eff}_-$ as a function of $[H_3O^+]$. Naturally, μ^{eff}_- is calculated by correcting the observed mobilities with the electroosmotic mobilities.

When $pH = pK_H + 3$, $[HR] \ll [R^-]$ and $[HS] \ll [S^-]$, then eqns. 13 and 14 become:

$$c_R = [R^-] + [RCD^-] \quad (52)$$

$$c_S = [S^-] + [SCD^-] \quad (53)$$

and with these, eqns. 19-22 simplify to:

$$\alpha^*_{R^-} = \frac{[R^-]}{[R^-] + [RCD^-]} = \frac{1}{1 + K_{RCD^-}[CD]} \quad (54)$$

$$\alpha^*_{S^-} = \frac{[S^-]}{[S^-] + [SCD^-]} = \frac{1}{1 + K_{SCD^-}[CD]} \quad (55)$$

$$\alpha^*_{RCD^-} = \frac{[RCD^-]}{[R^-] + [RCD^-]} = \frac{K_{RCD^-}[CD]}{1 + K_{RCD^-}[CD]} \quad (56)$$

$$\alpha^*_{SCD^-} = \frac{[SCD^-]}{[S^-] + [SCD^-]} = \frac{K_{SCD^-}[CD]}{1 + K_{SCD^-}[CD]} \quad (57)$$

Substitution into eqns. 23-24 yields:

$$\mu^{eff}_R = \mu^0_{R^-}\alpha^*_{R^-} + \mu^0_{RCD^-}\alpha^*_{RCD^-} = \frac{\mu^0_{R^-} + \mu^0_{RCD^-}K_{RCD^-}[CD]}{1 + K_{RCD^-}[CD]} \quad (58)$$

$$\mu^{eff}_S = \mu^0_{S^-}\alpha^*_{S^-} + \mu^0_{SCD^-}\alpha^*_{SCD^-} = \frac{\mu^0_{S^-} + \mu^0_{SCD^-}K_{SCD^-}[CD]}{1 + K_{SCD^-}[CD]} \quad (59)$$

If $K_{RCD^-}[CD] \gg 1$ and $K_{SCD^-}[CD] \gg 1$, and the CD concentration is close to saturation (18 mM), that is, the enantiomer anions are sufficiently strongly complexed by CD ($K_{RCD^-} \geq 500$), then eqns. 58 and 59 can be rearranged to yield:

$$\mu^{eff}_R = \frac{\mu^0_{R^-}}{K_{RCD^-}} \cdot \frac{1}{[CD]} + \mu^0_{RCD^-} \quad (60)$$

$$\mu^{eff}_S = \frac{\mu^0_{S^-}}{K_{SCD^-}} \cdot \frac{1}{[CD]} + \mu^0_{SCD^-} \quad (61)$$

Both $\mu^0_{RCD^-}$ and K_{RCD^-} can be determined by plotting μ^{eff}_R and μ^{eff}_S as a function of $1/[CD]$, because μ^0_- is known from the previous calculations. With these values K_{HRCD} and K_{HSCD} can be obtained explicitly from eqns. 27 and 28 as:

$$K_{HRCD} = \frac{K_H}{[H_3O^+][CD]\mu^{ef}_R} \cdot \left((\mu^0_- - \mu^{eff}_R) + K_{RCD^-}[CD](\mu^0_{RCD^-} - \mu^{eff}_R) - \frac{[H_3O^+]}{K_H}\mu^{eff}_R \right) \quad (62)$$

$$K_{HSCD} = \frac{K_H}{[H_3O^+][CD]\mu^{eff}_S} \cdot \left((\mu^0_- - \mu^{eff}_S) + K_{SCD^-}[CD](\mu^0_{SCD^-} - \mu^{eff}_S) - \frac{[H_3O^+]}{K_H}\mu^{eff}_S \right) \quad (63)$$

If, on the other hand, $K_{RCD^-}[CD] \ll 1$ and $K_{SCD^-}[CD] \ll 1$, while the CD concentration is close to saturation (18 mM), that is, the enantiomer anions are very weakly complexed by CD ($K_{RCD^-} \leq 5$), then eqns. 58 and 59 can be rearranged to yield:

$$\mu^{eff}_R = \mu^0_{R^-} + \mu^0_{RCD^-}K_{RCD^-}[CD] \quad (64)$$

$$\mu^{eff}_S = \mu^0_{S^-} + \mu^0_{SCD^-}K_{SCD^-}[CD] \quad (65)$$

from which the multiples $\mu^0_{RCD^-}K_{RCD^-}$ and $\mu^0_{SCD^-}K_{SCD^-}$ can be determined. Assuming that $[H_3O^+] \geq 100K_H$, and that $K_{HRCD}[CD] \gg 1$, substitution of these multiples into eqns. 27 and 28 results in eqns. 66 and 67,

$$\frac{\mu^{eff}_R[H_3O^+]}{K_H} = \frac{\mu^0_-}{K_{HRCD}} \cdot \frac{1}{[CD]} + \frac{\mu^0_{RCD^-}K_{RCD^-}}{K_{HRCD}} \quad (66)$$

$$\frac{\mu^{eff}_S[H_3O^+]}{K_H} = \frac{\mu^0_-}{K_{HSCD}} \cdot \frac{1}{[CD]} + \frac{\mu^0_{SCD^-}K_{SCD^-}}{K_{HSCD}} \quad (67)$$

which permit the determination of K_{HRCD} and K_{HSCD} from plots of the effective mobilities observed at low pH as a function of $1/[CD]$.

Once the ionic mobilities, the acid dissociation constants, and the complex formation constants are known, the effective mobilities of the individual enantiomers and the chiral selectivity of the given system can be calculated using eqns. 27 and 28 and 31. The calculated values then can be compared with the measured values to test the validity of the model proposed here. Also, the trends observed in these calculations can be used to predict the directions in which the background electrolyte parameters should be changed in order to achieve (or improve) a particular chiral CE separation.

EXPERIMENTAL

Two electrophoretic systems were used for these experiments. The first unit was built in our laboratory according to Jorgenson et al. [25] using a Model 200 variable UV detector (Linear Instruments, Reno, NV, USA), a Model PS/EH30R03.0 high-voltage power supply (Glassman, Whitehouse Station, NJ, USA), a custom-designed dual-loop liquid thermostatting system, a Perspex-glass safety box, a 1-kΩ resistor and an Omniscribe strip chart recorder (Industrial Scientific, Austin, TX, USA) to monitor the current during the separation, a Chrom-1 AT data acquisition board (Keithley-Metrabyte, Tauton, MA, USA) installed in a 386SX-20 NEC personal computer, and our ChromPlot1 data acquisition-data analysis software [26]. The second unit was a commercial electrophoretic instrument, a P/ACE 2100 system, equipped with a variable wavelength UV detector (Beckman Instruments, Fullerton, CA, USA). The electrode at the injection end of the capillary was kept at negative potential; the electrode at the detector end of the capillary was at ground potential.

Untreated, 25 μm I.D., 150 μm O.D. fused-silica capillaries (Polymicro Technologies, Phoenix, AZ, USA) were used in both systems (35 cm from injector to detector, 40 cm total length in the custom-built unit, 39 cm from injector to detector, 45.8 cm total length in the P/ACE unit). Before each and every series of measurements the capillaries were washed with 1 *M* NaOH, rinsed by deionized water and equilibrated by the background electrolyte (5 min, 5 min and 15 min, respectively).

The samples were injected electrokinetically; the injection and separation potentials were identical. The sample concentrations were kept at minimum (generally less than 0.1 m*M*) and the injection time was varied to insure similar sample loadings. In each run, a non-charged electroosmotic flow marker (a dilute solution of nitromethane) was injected at the detector end of the capillary at the same time that the sample was injected at the injection end, providing us with the accurate corrected mobilities. All separations were completed at a thermostatting liquid bath temperature of 37 °C. The UV detectors were set at 209 nm in the home-built unit and 214 nm in the P/ACE unit.

The field strength used for the separations was varied between 150 V/cm and 750 V/cm, depending on the actual conductivity of the background electrolyte. Power dissipation was kept in the 80 to 100 mW range to insure linear potential vs. current plots (Ohm-plots).

Native β-cyclodextrin was obtained from American Maize Products Corporation (Hammond, IN, USA). Reagent-grade morpholinoethanesulfonic acid monohydrate (MES), sodium hydroxide, racemic and *S*(+)-ibuprofen (IBU) were obtained from Aldrich (Milwaukee, WI, USA), racemic fenoprofen (FEN) from Sigma (St. Louis, MO, USA), 250MHR PA hydroxyethyl cellulose (HEC) from Aqualon Company (Wilmington, DE, USA). All chemicals were used as received without further purification. All solutions were freshly prepared using deionized water from a Millipore Q unit (Millipore, Milford, MA, USA). The background electrolytes were prepared by weighing the required amount of MES, CD and HEC into a volumetric flask. The flask was first filled with deionized water to 90% of its final capacity, stirred until all the components were dissolved, degassed, and made up almost to mark. Then the pH was adjusted to the desired value by adding a few μl of a 10 *M* NaOH solution and the flask was made up to mark with deionized water. The background electrolyte was degassed again prior to loading into the electrolyte reservoirs.

RESULTS AND DISCUSSION

In order to learn how chiral selectivity depends on the composition of the complex background electrolyte, and to test the validity of the model presented in the Theory section, the parameters were varied individually in small increments, over relatively broad ranges, while all the other parameters were kept constant providing a very precise description of both mobility and chiral selectivity.

The acid dissociation constants, K_H of fenoprofen and ibuprofen were determined using background electrolytes which contained 0.2%

(w/w) HEC and 200 m*M* MES. The pH of the background electrolyte was varied in the 4.1 to 7.1 range by adding NaOH. The effective mobilities of ibuprofen and fenoprofen, corrected for the electroosmotic flow, μ_-^{eff}, were determined in triplicate. The reciprocal effective mobilities are plotted in Figs. 1 and 2 as a function of the hydronium ion concentration according to eqn. 51, for a power load of 95 mW and thermostatting liquid temperature of 37°C.

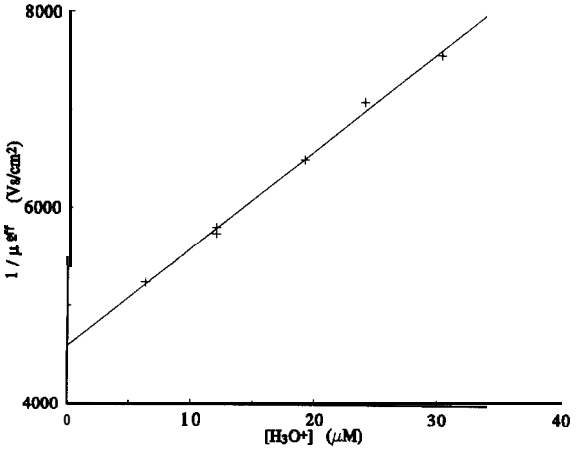

Fig. 1. Reciprocal effective mobility vs. hydronium ion concentration plot for fenoprofen in 200 m*M* MES, 0.2% HEC background electrolyte at a thermostatting liquid temperature of 37°C and power load of 95 mW. + = Measured values; solid line = least-square best fit line.

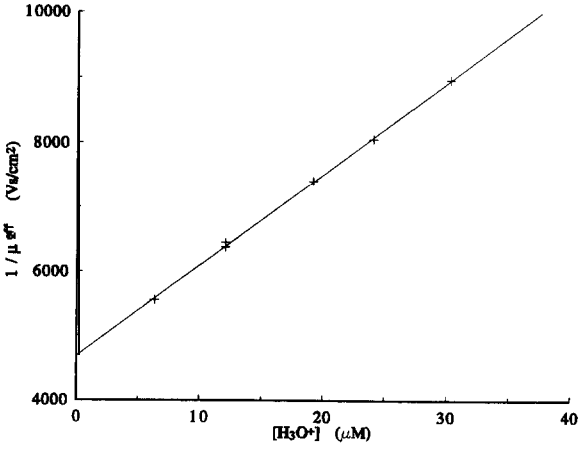

Fig. 2. Reciprocal effective mobility *vs.* hydronium ion concentration plot for ibuprofen. Conditions as in Fig. 1. + = Measured values; solid line = least-square best fit line.

The solid lines represent the least-square best fit lines. The ionic mobilities, μ_-^0, and acid dissociation constant values, Ku, are listed in the first four lines of Table III, along with the literature values of Ku determined at 25°C in pure aqueous solutions [27].

Because the background electrolytes used in these studies have a high concentration (in excess of 100 m*M*), accurate activity coefficient values cannot be calculated using the simple Debye–Hückel approach suggested by Becker-s *et* al. [28]. In addition, ibuprofen was reported to adsorb on hydroxyalkylated cellulose [29] dissolved in an electrolyte. Therefore, the acid dissociation constants determined in our measurements are concentration-based apparent dissociation constants, rather than thermodynamic, infinite dilution values. No ionic mobility values were found in the literature for fenoprofen and ibuprofen. However, the measured mobilities compare favorably with the ionic mobility of the structurally similar 4-*tert*.-butylbenzoic acid, $\mu_-^0 = 23.2 \cdot 10^{-5}\ cm^2/Vs$, as reported by Hirokawa et al. [30].

Next, the effects of cyclodextrin concentration were tested in a high-pH (pH = 7.1) background electrolyte in which both fenoprofen and ibuprofen were almost completely dissociated. When the effective mobilities were plotted against the reciprocal CD concentration accord-

TABLE III

IONIC MOBILITY AND APPARENT EQUILIBRIUM CONSTANT DATA FOR PENOPROFEN AND IBUPROFEN

Conditions as in Figs. 1 to 4.

Parameter	Fenoprofen	Ibuprofen
μ_-^0 (10^{-5} cm^2/Vs)	21.77 ± 0.03	21.32 ± 0.05
K_H	(4.57 ± 0.14) $\cdot 10^{-5}$	(3.31 ± 0.05). 10^{-5}
pK_H	4.34	4.48
pK_H 1271	4.50	5.10
$\mu^0_{RCD^-} = \mu^0_{SCD^-}$ (10^{-5} cm^2/Vs)	6.54 ± 0.05	6.60 ± 0.04
$K^0_{RCD^-} = K^0_{SCD^-}$	325 ± 7	1280 ± 5
K_{HRCD}	608 ± 18	1869 ± 48
K_{HSCD}	636 ± 20	1954 ± 49

ing to eqns. 60 and 61, estimates could be obtained for $\mu^0_{RCD^-}$, $\mu^0_{SCD^-}$, $K^0_{RCD^-}$ and $K^0_{SCD^-}$ from the limiting slopes and the intercepts. These estimates were then used to find the best fit between the measured values and the values calculated by eqns. 58 and 59. The $\mu^0_{RCD^-}$, $\mu^0_{SCD^-}$, $K^0_{RCD^-}$ and $K^0_{SCD^-}$ parameters obtained for both fenoprofen and ibuprofen are listed in Table III. The effective mobilities calculated by eqns. 58 and 59 and the best-fit parameters are shown in Figs. 3 and 4 as solid lines. The agreement between the measured and calculated values is very good.

Table III shows that the limiting ionic mobilities of the CD-complexed fenoprofen and ibuprofen are almost identical, in agreement with the observation that at high pH these complexed ions co-migrate. The complex formation constant for fenoprofen is almost four times lower than that of the ibuprofen. This relationship is reminiscent of the retention trend that were observed on β-cyclodextrin silica columns (Cyclobond I, ASTEC, Whippany, NJ, USA), when these columns were operated with high-pH eluents in the reversed-phase mode [23,31,32].

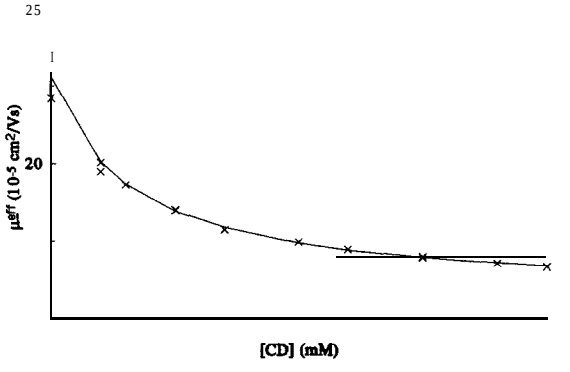

Fig. 3. Effective ionic mobility of fenoprofen as a function of the β-cyclodextrin concentration in a pH = 7.1 background electrolyte. Conditions as in Fig. 1. + = Measured values; solid line = calculated values using the parameters in Table III.

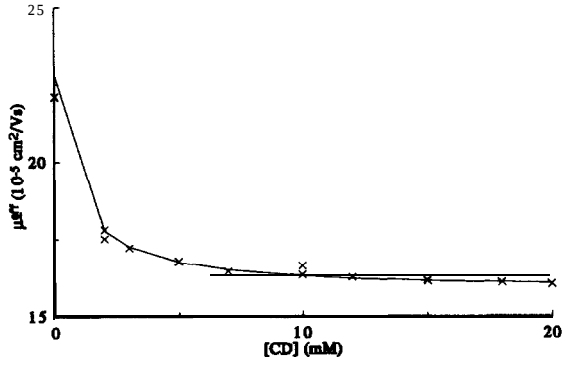

Fig. 4. Effective ionic mobilities of ibuprofen as a function of the β-cyclodextrin concentration in a pH = 7.1 background electrolyte. Conditions as in Fig. 1. + = Measured values; solid line = calculated values using the parameters in Table III.

Finally, a series of mobility measurements were carried out in a pH 4.52 background electrolyte in which both fenoprofen and ibuprofen are only partially dissociated. The CD concentration was varied between 0 and 18 m*M* while all other conditions were kept the same as in Figs. 3 and 4. In another series of measurements the CD concentration was kept constant at 15 m*M*, while the pH of the background electrolyte was varied between 4.0 and 5.6. The complex formation constants of the non-dissociated profen enantiomers (K_{HRCD}, K_{HSCD}) were calculated using the effective mobility values, eqns. 62 and 63, the respective parameters from the first six lines of Table III, and the actual [CD] and [H_3O^+] values. The results are listed in the last two lines of Table III. Interestingly, the complex formation constants of both protonated profens (K_{HRCD}, K_{HSCD}) are about two times larger than the respective complexation constants of the anions ($K^0_{RCD^-}$, $K^0_{SCD^-}$). This behavior is once again similar to what has been observed recently in the HPLC separation of profens on various cyclodextrin silica stationary phases, namely that in organic modifier-free eluents the protonated profens are retained more strongly than the respective anions [31,32].

In order to test the validity of the electrophoretic migration and chiral selectivity model presented here, the effective mobility and chiral selectivity values were calculated using eqns. 27, 28 and 31, the ionic mobilities, the acid dissociation constants, and the complex formation constants listed in Table III. The mobility data for fenoprofen and ibuprofen are compared with the measured values in Figs. 5 to 8, while the three-dimensional electrophoretic mobility surfaces are shown in Figs. 9 and 10. The chiral selectivity data for fenoprofen and ibuprofen are compared

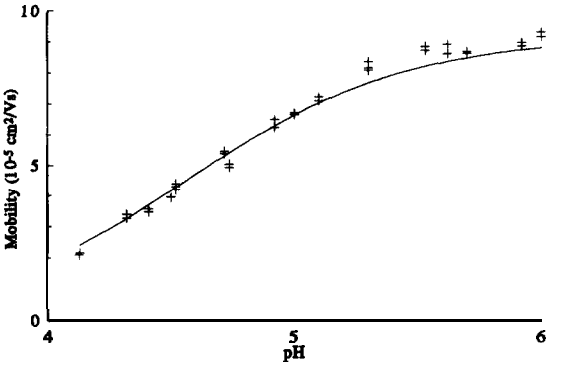

Fig. 5. Comparison of the measured and calculated effective mobilities for the more mobile enantiomer of fenoprofen as a function of the pH. Conditions as in Fig. 3, except [CD] = 15 m*M*. + = Measured values; solid line = calculated values using eqn. 27 and the parameters in Table III.

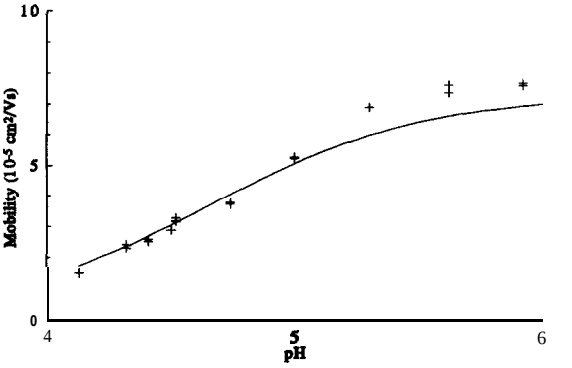

Fig. 7. Comparison of the measured and calculated effective mobilities for the more mobile enantiomer of ibuprofen as a function of the pH. Conditions as in Fig. 3, except [CD] = 15 m*M*. + = Measured values; solid line = calculated values using eqn. 27 and the parameters in Table III.

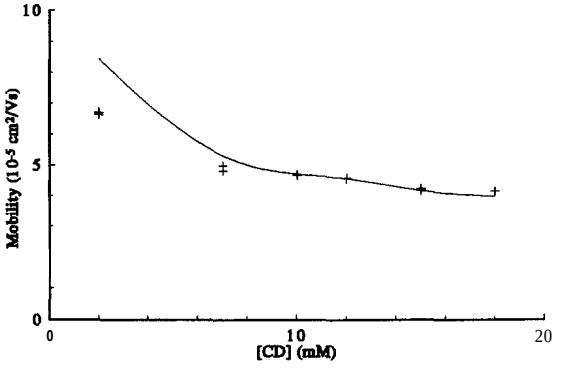

Fig. 6. Comparison of the measured and calculated effective mobilities for the more mobile enantiomer of fenoprofen as a function of the CD concentration. Conditions as in Fig. 3, except 4.50 < pH < 4.53. + = Measured values; solid line = calculated values using eqn. 27 and the parameters in Table III.

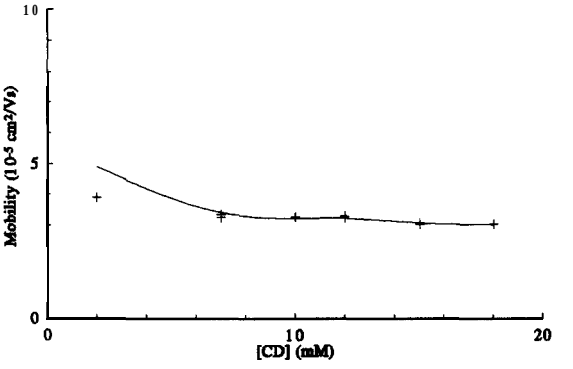

Fig. 8. Comparison of the measured and calculated effective mobilities for the more mobile enantiomer of ibuprofen as a function of the CD concentration. Conditions as in Fig. 3, except 4.50 < pH < 4.53. + = Measured values; solid line = calculated values using eqn. 27 and the parameters in Table III.

with the measured values in Figs. 11 to 14, while the three-dimensional selectivity surfaces are shown in Figs. 15 and 16.

In all the plots the symbol + stands for the measured values while the continuous line represents the calculated values. It can be seen from Figs. 5-8 and 11-14 that the agreement between the measured and the calculated values is indeed excellent.

The electrophoretic mobility surface is shown from two different viewpoints for fenoprofen (Fig. 9) and ibuprofen (Fig. 10). It can be seen that the surface is strongly curved for both solutes: the mobility decreases rapidly as CD is added to the background electrolyte, but then it levels off above [CD] = 10 m*M*. On the pH axis, most of the mobility change occurs in the $pK_H - 1 < pH < pK_H + 1$ range (where the mobility surface is shaped like a regular mole fraction function).

In the pH > 5.5 range, the calculated selectivity values seem to be slightly higher than the measured values (Figs. 11 and 13). This is due to the fact that in the actual electropherograms the peaks of the enantiomers are no longer resolved when the chiral selectivity decreases below

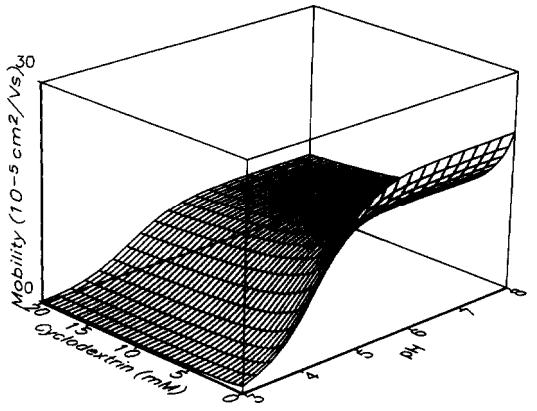

Fig. 9. Three-dimensional effective mobility surface for the more mobile enantiomer of fenoprofen as a function of the CD concentration and the pH, calculated using eqn. 27 and the parameters in Table III.

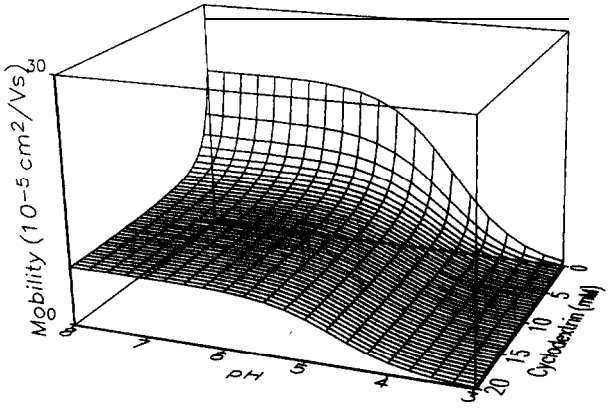

Fig. 10. Three-dimensional effective mobility surface for the more mobile enantiomer of ibuprofen as a function of the CD concentration and the pH, calculated using eqn. 27 and the parameters in Table III.

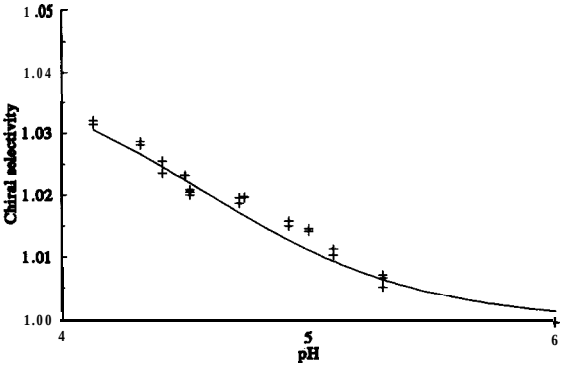

Fig. 11. Comparison of the measured and calculated chiral selectivities for fenoprofen as a function of the pH. Conditions as in Fig. 5. + = Measured values; solid line = calculated values using eqn. 31 and the parameters in Table III.

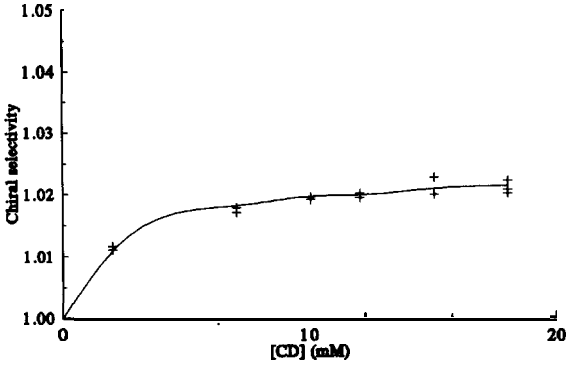

Fig. 12. Comparison of the measured and calculated chiral selectivities for fenoprofen as a function of the CD concentration. Conditions as in Fig. 6. + = Measured values; solid line = calculated values using eqn. 31 and the parameters in Table III.

1.005, resulting in an assigned selectivity of unity. It can be seen from the selectivity surfaces of both fenoprofen (Fig. 15) and ibuprofen (Fig. 16), shown again from two different viewpoints, that both profens belong to the family of Type I enantiomers: chiral selectivities vary monotonously between their pH and CD concentration dependent high values and unity, and the migration order of the enantiomers cannot be reversed by varying either the CD concentration or the pH, or both.

It can be also seen that chiral selectivity increases more rapidly with the CD concentration for ibuprofen than for fenoprofen. The limiting chiral selectivity that can be achieved at pH = 3 and [CD] = 20 m*M* is slightly higher for ibuprofen than for fenoprofen. Both of these trends are due to the fact that the complexation constants of both the ionic and the protonated forms of fenoprofen are about three times smaller than those of the ibuprofen.

By considering the shapes of both the mobility and the selectivity surfaces of the profens, one may conclude that the best strategy to optimize the separation would call for CD concentrations that are close to the solubility limit (15 m*M* is safe) and background electrolyte pH values that

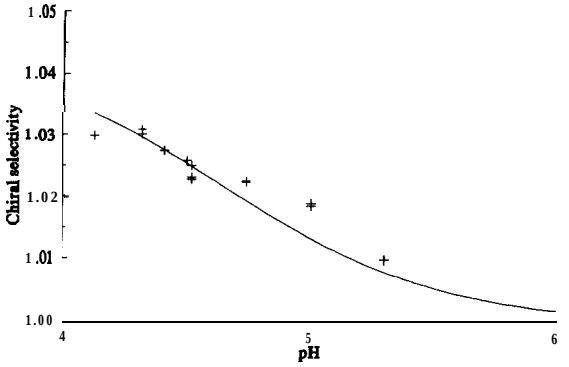

Fig. 13. Comparison of the measured and calculated chiral selectivities for ibuprofen as a function of the pH. Conditions as in Fig. 5. + = Measured values; solid line = calculated values using eqn. 31 and the parameters in Table III.

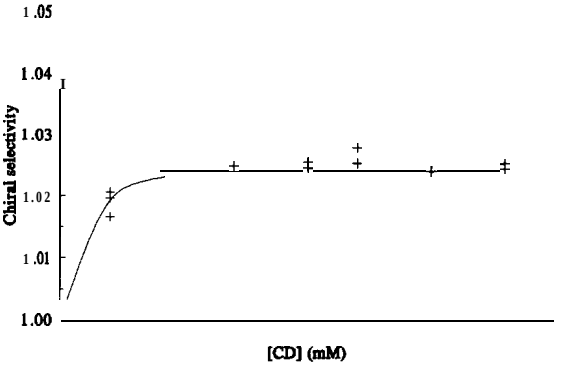

Fig. 14. Comparison of the measured and calculated chiral selectivities for ibuprofen as a function of the CD concentration. Conditions as in Fig. 6. + = Measured values; solid line = calculated values using eqn. 31 and the parameters in Table III.

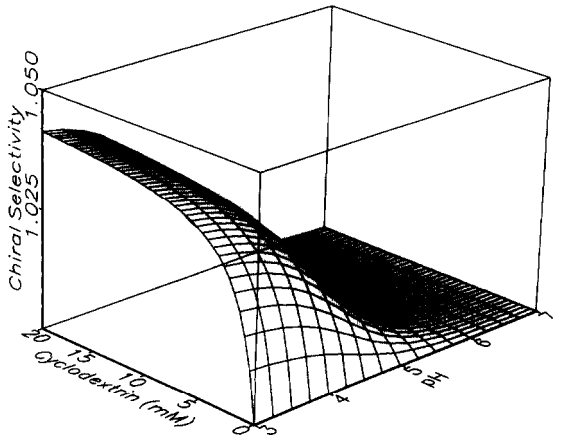

Fig. 15. Three-dimensional chiral selectivity surface for fenoprofen as a function of the CD concentration and the pH, calculated using eqn. 31 and the parameters in Table III.

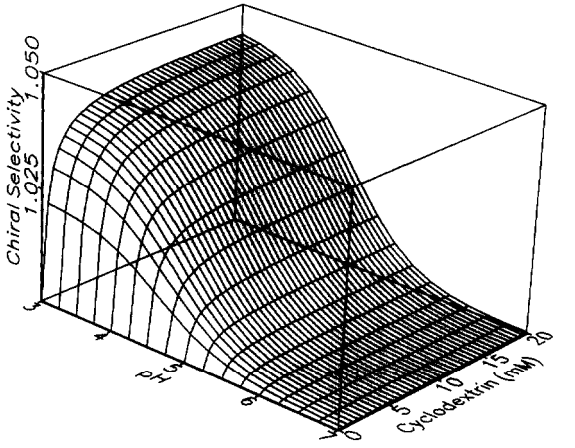

Fig. 16. Three-dimensional chiral selectivity surface for ibuprofen as a function of the CD concentration and the pH, calculated using eqn. 31 and the parameters in Table III.

are not any lower than necessary to achieve the desired minimum selectivity (minimum resolution), and pay as little a migration time penalty as possible.

The electropherogram of a mixture of racemic fenoprofen and ibuprofen is shown in Fig. 17. Baseline separations of the enantiomers can be achieved with 15 m*M* CD at pH 4.5 in about half an hour.

CONCLUSIONS

An equilibrium model has been developed to describe the electrophoretic mobilities of the enantiomers of chiral weak acids and the resulting chiral separation selectivities, as a function of the pH and the cyclodextrin concentration of the background electrolyte. The parameters of the model can be readily derived from three sets of specifically designed separation experiments: one at varying pH values without cyclodextrin in the background electrolyte, one at high pH with varying concentrations of cyclodextrin, and one at low pH with varying concentrations of

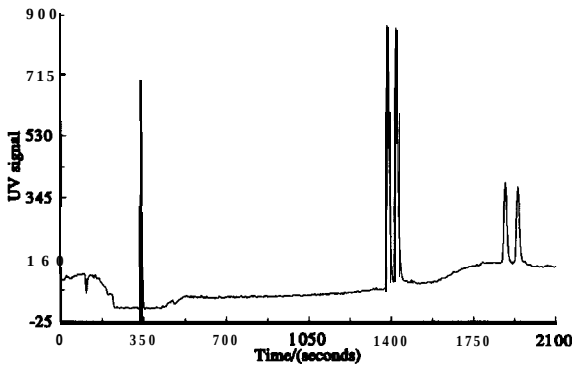

Fig. 17. CE separation of the enantiomers of fenoprofen and ibuprofen. Conditions: 0.2% HEC, 200 m*M* MES, pH = 4.50, [CD] = 15 m*M*.

cyclodextrin in the background electrolyte. The validity of the model has been demonstrated by comparing the measured and the calculated values for two test probes, fenoprofen and ibuprofen.

Fenoprofen and ibuprofen behave with β-cyclodextrin as Type I solutes defined in the Theory, because their chiral selectivity varies monotonously with both the pH and the CD concentration, the migration order of the enantiomers cannot be reversed by varying either the pH or the CD concentration of the background electrolyte, or both, and chiral resolution is absent in high pH electrolytes.

Further work is under way in our laboratory to extend the migration and chiral selectivity model proposed here to other solute types as well.

ACKNOWLEDGEMENTS

Partial financial support of this project by the National Science Foundation (CHE-8919151), the Dow Chemical Company (Midland, MI, USA), Genentech (South San Francisco, CA, USA) and Beckmann Instruments (Fullerton, CA, USA) is gratefully acknowledged. The authors are also indebted to Beckman Instruments for the loan of the P/ACE 2100 instrument. American Maize Products Corporation (Hammond, IN, USA) and the Aqualon Corporation (Wilmington, DE, USA), respectively, are acknowledged for the donation of the cyclodextrin and hydroxyethyl cellulose samples used in this project.

REFERENCES

1 W.L. Hinze, Sep. *Purif. Meth.*, 10 (1981) 159.
2 G. Gubitz, *Chromatographia*, 30 (1990) 555.
3 V. Schurig and H.P. Nowotny, *J.* Chromatogr., 441 (1988) 155.
4 S. Terabe, H. Ozaki and T. Ando, *J. Chromatogr.*, 348 (1985) 39.
5 J. Liu, K.A. Cobb and M. Novotny, *J.* Chromatogr., 519 (1990) 189.
6 H. Nishi, T. Fukuyama and S. Terabe, *J. Chromatogr.*, 553 (1991) 503.
7 I. Jelinek, J. Snopek and E. Smolková-Keulemansová, *J.* Chromarogr., 405 (1987) 379.
8 J. Snopek, I. Jelinek and E. Smolková-Keulemansová, *J. Chromatogr.*, 411 (1987) 153.
9 1. Jelinek, J. Dohnal, J. Snopek and E. Smolková-Keulemansová, *J. Chromatogr.*, 435 (1988) 4%.
10 J. Snopek, I. Jelinek and E. Smolková-Keulemansová, *J.* Chromutogr., 438 (1988) 211.
11 I. Jelinek, J. Snopek and E. Smolková-Keulemansová, *J.* Chromatogr., 439 (1988) 386.
12 S. Fanali and M. Sinibaldi, *J.* Chromatogr., 442 (1988) 371.
13 J. Snopek, E. Smolková-Keulemansová, I. Jelfnek, J. Dohnal, J. Klinot and E. Klinotová, *J.* Chromatogr., 450 (1988) 373.
14 I. Jelinek, J. Dohnal, J. Snopek and E. Smolková-Keulemansovl, *J. Chromatogr.*, 464 (1989) 139.
15 J. Snopek, I. Jelfnek and E. Smolková-Keulemansová, *J.* Chromatogr., 472 (1989) 308.
16 I. Jelinek, J. Snopek, J. Dian and E. Smolkovh Keulemansovl, *J.* Chromarogr., 470 (1989) 113.
17 I. Jelinek, J. Snopek and E. Smolková-Keulemansová, *J. Chromatogr.*, *557* (1991) 215.
18 S. Fanali, *J. Chromatogr., 474 (1989)* 441.
19 S. Fanali, *J. Chromatogr., 545* (1991) 437.
20 J. Snopek, H. Soini, M. Novotny, E. Smolková-Keulemansová and I. Jelinek, *J. Chromarogr., 559* (1991) 215.
21 A. Guttman, A. Paulus, A.S. Cohen, N. Grinberg and B.L. Karger, *J. Chromarogr., 448 (1988) 41.*
22 I. Cruzado and Gy. Vigh, *J. Chromatogr., 608* (1992) 421.
23 Gy. Vigh, G. Quintero, Gy. Farkas, in Cs. Horváth and J. Nikely (Editors), *Analytical Biotechnology, American* Chemical Society, Washington, DC, 1990, p. 181.
24 J.W. Jorgenson and K.D. Lukacs, *Anal. Chem.*, 53 (1981) 1298.
25 J.W. Jorgenson and K.D. Lukacs, Science *(Washington, DC), 222 (1983) 266.*
26 Gy. Vigh, Gy. Farkas and G. Quintero, *J. Chromatogr., 495* (1990) 219.

27 C.D. **Herzfeldt** and R. **Kummel**, *Drug Dev. Ind. Pharm.*, 9 (1983) 767.
28 J.L. **Beckers**, F.M. Everaerts and M.T. **Ackermans**, *J. Chromatogr., 537* (1991) **407**.
29 S.L. Law, *T'ai-wan Yao Hsueh Tsa Chih, 36 (1984) 173.*
30 T. Hirokawa, M. Nishino, N. Aoki, Y. Kiso, I. **Sawa**-moto, T. Yagi and J.-I. Akiyama, ***J.*** Chromatogr., 271 (1983) **D1–D106**.
31 M.D. **Beeson** and Gy. Vigh, ***J. Chromatogr., 634 (1993)*** 197.
32 Gy. Farkas, G. Quintero, L.H. Irgens and Gy. Vigh, ***J. Chromatogr., (1993)*** submitted.